View metadata, citation and similar papers at core.ac.uk

brought to you by CORE

provided by Explore Bristol Research

Sun, H., Simon, R. B., Pomeroy, J. W., Francis, D., Faili, F., Twitchen, D. J., & Kuball, M. H. H. (2015). Reducing GaN-on-diamond interfacial thermal resistance for high power transistor applications. Applied Physics Letters, 106(11), [111906]. 10.1063/1.4913430

Peer reviewed version

Link to published version (if available):
10.1063/1.4913430

Link to publication record in Explore Bristol Research

PDF-document

University of Bristol - Explore Bristol Research

General rights

This document is made available in accordance with publisher policies. Please cite only the published version using the reference above. Full terms of use are available: http://www.bristol.ac.uk/pure/about/ebr-terms.html

Take down policy

Explore Bristol Research is a digital archive and the intention is that deposited content should not be removed. However, if you believe that this version of the work breaches copyright law please contact open-access@bristol.ac.uk and include the following information in your message:

• Your contact details
• Bibliographic details for the item, including a URL
• An outline of the nature of the complaint

On receipt of your message the Open Access Team will immediately investigate your claim, make an initial judgement of the validity of the claim and, where appropriate, withdraw the item in question from public view.

Reducing GaN-on-diamond interfacial thermal resistance for high power transistor applications

Huarui Sun,[1, a)] Roland B. Simon,[1] James W. Pomeroy,[1] Daniel Francis,[2] Firooz Faili,[2] Daniel J. Twitchen,[2] and Martin Kuball[1]
[1]*Center for Device Thermography and Reliability (CDTR), H. H. Wills Physics Laboratory, University of Bristol, Tyndall Avenue, Bristol BS8 1TL, United Kingdom*
[2]*Element Six Technologies U.S. Corporation, Santa Clara, CA 95054, USA*

Integration of chemical vapor deposited (CVD) polycrystalline diamond offers promising thermal performances for GaN-based high power radio frequency (RF) amplifiers. One limiting factor is the thermal barrier at the GaN to diamond interface, often referred to as the effective thermal boundary resistance (TBR_{eff}). Using a combination of transient thermoreflectance measurement, finite element modeling and microstructural analysis, the TBR_{eff} of GaN-on-diamond wafers is shown to be dominated by the SiN_x interlayer for diamond growth seeding, with additional impacts from the diamond nucleation surface. By decreasing the SiN_x layer thickness and minimizing the diamond nucleation region, TBR_{eff} can be significantly reduced, and a TBR_{eff} as low as 12 m^2K/GW is demonstrated. This enables a major improvement in GaN-on-diamond transistor thermal resistance with respect to GaN-on-SiC wafers. A further reduction in TBR_{eff} towards the diffuse mismatch limit is also predicted, demonstrating the full potential of using diamond as the heat spreading substrate.

As the power density in GaN-based high electron mobility transistors (HEMTs) rises, heat removal near the junction becomes increasingly important for device performance and reliability. The thermal conductivity of SiC (~ 450 W/m-K) as a standard substrate material is still a limiting factor in device thermal performance and must be taken into account in device designs. Chemical vapor deposited (CVD) polycrystalline diamond has a high thermal conductivity that can reach up to 2000 W/m-K[1] and is therefore being developed as a superior heat spreading substrate for GaN devices. The latest GaN-on-diamond technology has already demonstrated its scalability[1] and promising electrical[2,3] and thermal performance[4,5] for RF transistors.

For GaN-on-diamond wafers, the heat spreading capability is determined not only by the diamond thermal conductivity ($\kappa_{diamond}$) but also the effective thermal boundary resistance (TBR_{eff}) at the GaN to diamond interface. This TBR_{eff} is in general associated with the acoustic mismatch between materials, the dielectric interlayer used for diamond growth seeding, and the defective transition region near the nucleation surface (referred to as the nucleation layer). Measured GaN-on-diamond TBR_{eff} ranges from 10 to 50 m^2K/GW,[6,7] values competitively low in comparison with GaN-on-SiC[8-10] and GaN-on-Si wafers.[10,11] However, this TBR_{eff} still constitutes a significant proportion of the overall wafer thermal resistance[4] and needs to be minimized to fully exploit the benefit of the diamond substrate; a complete understanding of its physical origins is therefore crucial. In this letter, we study a series of as-grown GaN-on-CVD diamond wafers fabricated with different seeding layer thicknesses and growth methods using a fully contactless transient thermoreflectance technique recently developed,[12] to correlate thermal properties, material structures and interface features characterized by transmission electron microscopy (TEM). Understanding of contributions of individual components to the overall wafer thermal resistance is provided, delivering insight into how to exploit the thermal benefit of GaN-on-diamond device wafers.

The GaN-on-diamond wafers investigated were prepared using a procedure described in Ref. 2. An AlGaN/GaN heterostructure grown on Si substrates by metal-organic CVD was used as the starting material. The GaN-on-Si wafer was temporarily mounted on a handle wafer, after which the Si substrate and nitride strain relief layers were removed. A thin amorphous SiN_x layer was subsequently deposited onto the exposed GaN using low-pressure CVD, for the seeding of the CVD growth of a 100 μm-thick polycrystalline diamond. Two diamond growth methods were used: Hot filament (HF) CVD and microwave (MW) plasma CVD. The appearance of the HF and MW diamond wafers was opaque and translucent, respectively. A total of 17 wafers were studied, each having a GaN thickness of 0.7 - 1 μm and a SiN_x layer thickness in a range between 28 and 100 nm.

For the transient thermoreflectance measurement, a 355 nm frequency-tripled Nd:YAG laser (3.49 eV, i.e. above GaN bandgap) with a pulse duration of 10 ns and a spot size of 90 μm is used as a heating pulse to induce a rapid temperature rise at the surface of the AlGaN/GaN. This modulates the refractive index that is linearly dependent on temperature.[13] A continuous wave (CW), 532 nm frequency-doubled Nd:YAG laser with a spot size of 2 μm is used to monitor the change in surface reflectance, and therefore temperature rise. The contrast in the refractive index of each layer ($n_{air} = 1$, $n_{GaN} \approx 2.4$, $n_{SiN_x} \approx 2$, and $n_{diamond} \approx 2.4$ at 532 nm) makes this measurement

[a)] Electronic mail: huarui.sun@bristol.ac.uk

particularly effective for GaN-on-diamond, as the dominant reflection occurs at the AlGaN/GaN surface. The use of a CW probe laser enables a measurement window of up to 33 μs (corresponding to the 30 kHz pump laser repetition rate), considerably wider than for example picosecond laser-based time domain thermoreflectance (usually less than 10 ns).[7,9,10] A long measurement range is essential to GaN-on-diamond wafers, given the thermal relaxation time of the layer structure being up to microseconds. A schematic of the measurement is shown as an inset of FIG. 1, with more details of the technique described in Ref. 12.

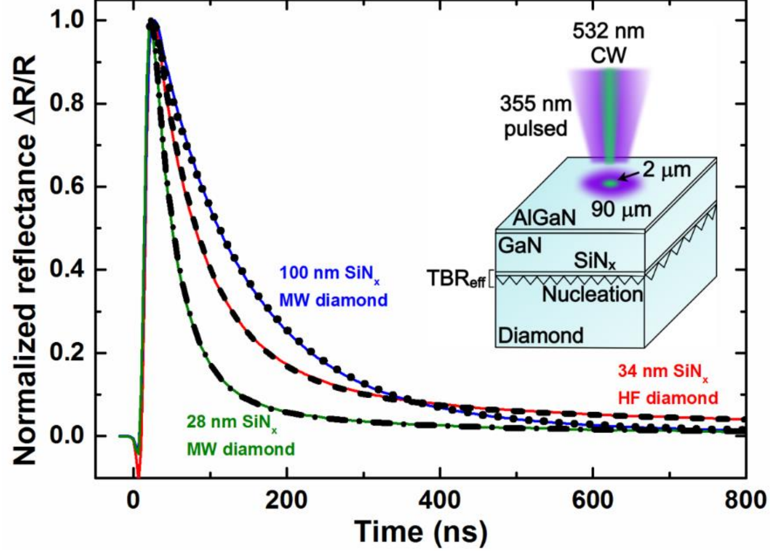

FIG. 1. Normalized transient thermoreflectance measured on three GaN-on-diamond wafers with 100 nm, 34 nm and 28 nm-thick SiN_x layers on either the opaque hot filament (HF) CVD diamond or the translucent microwave (MW) plasma CVD diamond. Best fit curves are overlaid with results given in TABLE I. Inset shows a schematic of the measurement.

FIG. 1 shows the normalized transient reflectance change of three selected wafers with different thicknesses of the SiN_x layer, and different CVD diamond growth methods, illustrating the corresponding temperature transient at the AlGaN/GaN surface in each case. The reflectance change peaks after the laser pulse heating, and then experiences a gradual decay due to heat diffusion into the GaN layer and diamond substrate. The small negative peak near time zero is caused by the non-equilibrium excitation of hot electrons, which rapidly relax their energy to the lattice through electron-phonon coupling.[14] The time constant of thermal relaxation is clearly reduced with a thinner SiN_x interlayer, illustrating the effect of a lowered TBR_{eff}. On long timescales, there is a difference in the transients between the two types of diamonds (HF, MW). The reflectance signals of the translucent MW diamond samples both converge to a value lower than that of the opaque HF diamond sample at 800 ns, due to the difference in the thermal conductivity of the two diamond substrates.

To extract the different contributions to the thermal resistance of GaN-on-diamond from the measurement, a three-dimensional finite element model was employed to simulate the temperature transients and fit to the measurement results. Fixed input parameters of this model include the thickness of the GaN and the diamond substrate, the thermal conductivity of GaN,[15] the specific heat of GaN[16] and diamond,[17] as well as the laser pulse duration and spot size, with the remainder i.e. $\kappa_{diamond}$ and TBR_{eff} treated as free parameters in fitting the experimental data. TBR_{eff} included contributions from the thin SiN_x interlayer and the initial nucleation layer of diamond growth (usually < 50 nm). The thin AlGaN layer on the surface of the HEMT was neglected in the simulation as it had no sizable effect on the thermal simulation results.

TABLE I. Fit model results of $\kappa_{diamond}$ and TBR_{eff}.

	$\kappa_{diamond}$ (W/m-K)	TBR_{eff} (m^2K/GW)
34 nm SiN_x Opaque HF diamond	620 ± 50	25 ± 3
100 nm SiN_x Translucent MW diamond	1500 ± 300	50 ± 5
28 nm SiN_x Translucent MW diamond	1500 ± 300	12 ± 2

Based on the simulated transients, the effect of heat diffusion within the sub-μm thick GaN layer only takes place in the first 60 ns (for brevity not shown). In general, the interface dominates the characteristics within about 50 – 400 ns and the diamond substrate governs the long-time thermal behavior (> 300 ns). This allows reasonably independent determination of the effective $\kappa_{diamond}$ and TBR_{eff} from the measurement results. The least-square fit

curves of the three wafers are presented in FIG. 1 with fit parameters listed in TABLE I. The results first show the higher thermal conductivity of the translucent MW diamond compared to the opaque HF diamond, and secondly, illustrates that TBR_{eff} is strongly dependent on the thickness of the SiN_x layer (d_{SiN_x}). The extracted diamond thermal conductivities are consistent with reported values for similar HF and MW diamonds measured using Raman thermography on full AlGaN/GaN-on-diamond HEMT structures.[4] It is known that the thermal conductivity of CVD polycrystalline diamond increases from the nucleation site along the growth direction due to the gradual increase in crystal grain size.[18] $\kappa_{diamond}$ in the thermal model represents a depth-wise weighted average over the 100 μm thickness of the diamond wafer, excluding the thin nucleation layer which is included in TBR_{eff}.

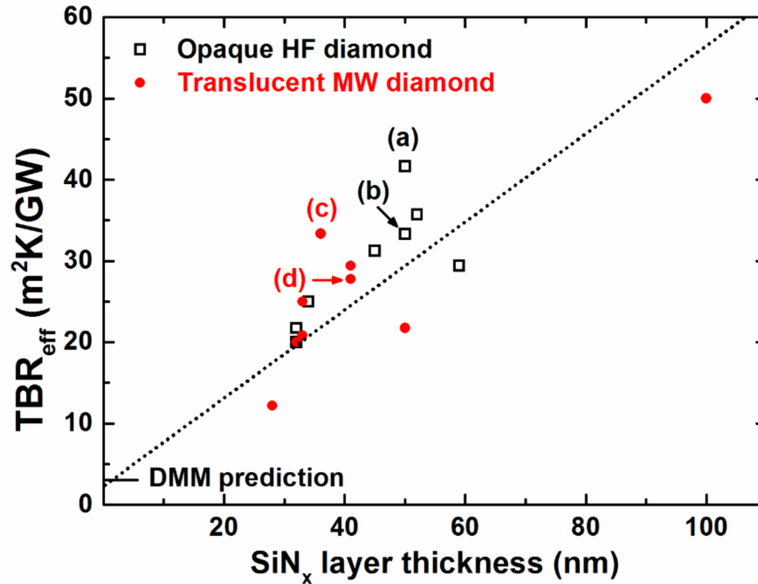

FIG. 2. Effective thermal boundary resistance (TBR_{eff}) of GaN-on-diamond wafers as a function of the SiN_x layer thickness. The data points broadly follow a fit straight line and the thermal conductivity of the amorphous SiN_x layer is estimated to be 1.9 ± 0.4 W/m-K from the slope. The diffuse mismatch model (DMM) prediction for the minimum possible TBR_{eff} is indicated. Labeled are wafers selected for TEM imaging in FIG. 3.

FIG. 2 summarizes the extracted TBR_{eff} values of the series of wafers studied. Assuming a thermal conductivity for the SiN_x layer independent of the layer thickness and temperature, a valid assumption for amorphous materials, the total GaN-on-diamond interfacial thermal resistance can be written as: $TBR_{eff} = d_{SiN_x} / \kappa_{SiN_x} + R_0$, where κ_{SiN_x} is the thermal conductivity of the SiN_x layer, and R_0 represents the sum of the thermal resistances of the thin diamond nucleation layer, and the GaN/SiN_x and SiN_x/diamond boundaries. The observed dependence of TBR_{eff} as a function of d_{SiN_x} shown in FIG. 2 is consistent with this anticipated linear relationship. Using the inverse of the slope of the linear fit, κ_{SiN_x} is estimated to be 1.9 ± 0.4 W/m-K, consistent with what is expected for amorphous silicon nitride thin films.[19-21] This low thermal conductivity layer is a bottle neck for heat transfer and needs to be minimized to take the fullest advantage of the heat sinking capability of diamond. While the bulk thermal conductivity of the opaque HF diamond is lower than that of the translucent MW diamond, TBR_{eff} values for the two diamonds appear to follow a similar distribution near the fit straight line. This suggests that the near-junction diamond thermal conductance is statistically comparable for the two diamonds if we neglect temporarily the differences between individual wafers (a point addressed next). Extrapolating the SiN_x layer thickness to zero gives a TBR_{eff} value below 7 m^2K/GW, taken into account the uncertainty of the linear fit. This gives an approximate range for the minimum possible TBR_{eff}, R_0, which is discussed later in more detail.

While the d_{SiN_x} dependence of TBR_{eff} in FIG. 2 follows broadly a linear relationship, apparent is a scatter of the data points. This is caused by variations in the diamond nucleation region in each wafer. To examine the effect of the nucleation interface on TBR_{eff}, selected wafers (see labeled points in FIG. 2) were imaged using cross-sectional TEM shown in FIG. 3, representing substantial differences in the initial nucleation region in each of the diamonds. The nucleation region in general contains a higher concentration of impurities, defects and grain boundaries and thus leads to a lower thermal conductance due to enhanced phonon scattering. Initially we focus on the two HF diamond GaN samples; an estimated 50 nm-thick nucleation layer (darker area in FIG. 3(a)) is evident for Sample (a) with a TBR_{eff} of 42 m^2K/GW, whereas for Sample (b) with a TBR_{eff} of 33 m^2K/GW this layer is only 20 nm thick (FIG. 3(b)). From the difference in the TBR_{eff} between these two samples, the thermal conductivity of the nucleation layer is estimated to be ~ 3 W/m-K, 200× lower than the effective thermal conductivity measured of

the bulk HF diamond. This is in line with reported values for nanocrystalline diamond near the nucleation surface.[22,23] For the two MW diamond GaN samples; a nucleation layer is visible with nanocrystal grains near the junction, as seen in FIG. 3(c) and (d). Although Sample (c) has a thinner SiN_x layer, it has a 20% higher TBR_{eff} compared to Sample (d) with a thinner nucleation layer, highlighting the contribution of the nanocrystalline nucleation region to TBR_{eff}. It is also worth comparing for example Sample (b) on the HF diamond and Sample (c) on the MW diamond. Sample (c) despite its smaller nominal SiN_x thickness has a similar TBR_{eff} to Sample (b). This is likely due to the thicker nucleation layer in (c), and additionally, to the thinned SiN_x layer during the HF diamond growth evident in FIG. 2(a) and (b). The examples shown in FIG. 3 demonstrate the impact of the nanostructures near the diamond nucleation interface on TBR_{eff}, which causes the scattered behavior of data points in FIG. 2. For either of the diamond growth methods, the defective nucleation layer needs to be reduced as far as possible to ensure a low interfacial thermal resistance.

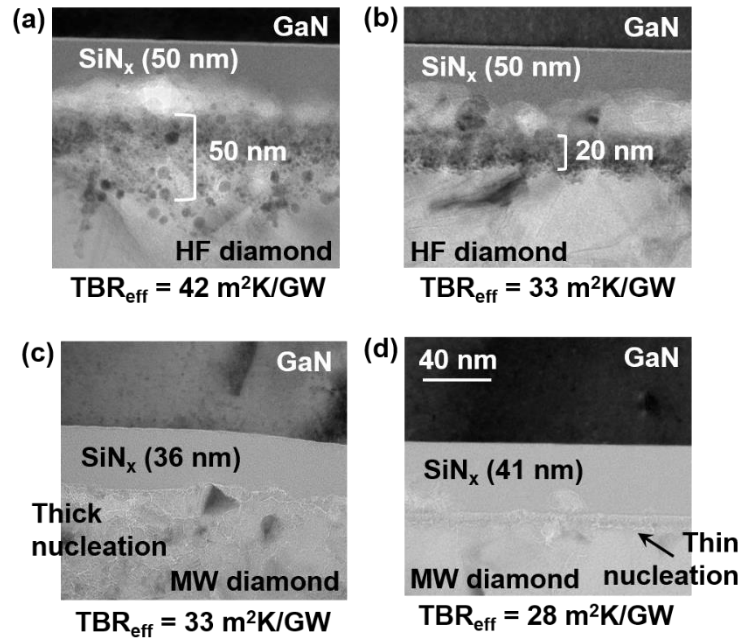

FIG. 3. Cross-sectional TEM images of representative (a)(b) opaque HF and (c)(d) translucent MW diamond wafers, showing the microstructures near the GaN to diamond interfaces. The corresponding TBR_{eff} values are also indicated in FIG. 2.

Given that the thickness of the nucleation layer is sample-to-sample dependent (FIG. 3), R_0 as an onset of TBR_{eff} should vary in each wafer, and this variation inevitably enters the $TBR_{eff} - d_{SiN_x}$ correlation in FIG. 2. Consequently, uncertainties arise in the vertical intercept and slope extracted in FIG. 2 due to the single line fitting. Nonetheless, the effective R_0 determined here is on the same order as the thermal boundary resistance (3 m^2K/GW) between GaN and diamond predicted by the diffuse mismatch model (DMM),[24] i.e. assuming a structurally perfect GaN to diamond interface which is the minimum possible interfacial thermal resistance. The fact that TBR_{eff} approaches the DMM prediction suggests that GaN-on-diamond wafers have the potential to reach the maximum thermal benefit of diamond if the SiN_x interlayer could be removed.

It should be noted that all measurements were performed at room temperature (25 °C), although a temperature rise within the layer structure is present due to the UV pulse laser heating. Using the thermal simulation, the surface temperature is estimated to be up to 75 °C at the peak of the laser pulse. The corresponding temperature at the GaN to diamond interface varies between 30 °C and 65 °C in time and depth; TBR_{eff} measured here is effectively an average value over this temperature range. Nevertheless, the temperature deviation among all wafers is estimated to be less than 10 °C, which should have a negligible effect on the measured TBR_{eff} from wafer to wafer.

To illustrate the device thermal performance in terms of the measured $\kappa_{diamond}$ and TBR_{eff}, a finite element transistor thermal model was built based on an 10×125 μm wide, 33 μm gate pitch HEMT with a layer structure shown in FIG. 1 and a heat dissipation of 5 W/mm. The corresponding peak channel temperature rise (ΔT_{peak}) was calculated as a function of TBR_{eff} for three different substrates: SiC (450 W/m-K), the opaque HF diamond (620 W/m-K) and translucent MW diamond (1500 W/m-K) measured here, giving a quantitative assessment of the device thermal resistance. The GaN-on-diamond TBR_{eff} obtained has a similar range as reported TBR_{eff} for GaN-on-SiC wafers.[8] As illustrated in FIG. 4, both the substrate thermal conductivity and TBR_{eff} greatly affect ΔT_{peak};

the percentage of drop in ΔT_{peak} by reducing TBR_{eff} is more pronounced for the MW diamond compared to SiC and the HF diamond, highlighting the important role of TBR_{eff} for high thermal conductivity substrates. The GaN-on-MW diamond is expected to result in a ΔT_{peak} ~ 40% lower than GaN-on-SiC at a given TBR_{eff}. This permits a ~ 3× increase in output power density at the same ΔT_{peak} for transistors on the MW diamond with respect to transistors on SiC by reducing the gate pitch three times. Future improvements are possible with further reductions in GaN-on-diamond TBR_{eff} as predicted in FIG. 2.

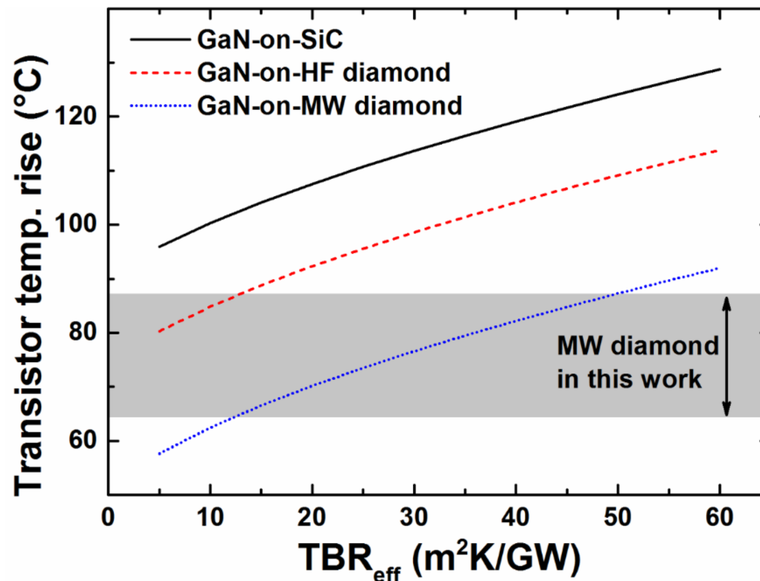

FIG. 4. Simulated peak channel temperature rise of a multi-finger AlGaN/GaN HEMT on different device wafers. The range of temperature rise corresponding to the GaN-on-MW diamond wafers characterized in this work is indicated.

In conclusion, we have presented a detailed analysis of the different contributions to the total thermal resistance of GaN-on-diamond wafers. The diamond thermal conductivity and interfacial thermal resistance were simultaneously determined for a series of as-grown GaN-on-diamond wafers using a fully contactless transient thermoreflectance technique. An effective thermal conductivity of 620 ± 50 W/m-K and 1500 ± 300 W/m-K was extracted for the opaque hot filament CVD diamond and translucent microwave plasma CVD diamond, respectively. To a great extent, the GaN-on-diamond interfacial thermal resistance scales with the thickness of the SiN_x layer for diamond growth seeding, with further contributions from the transition region near the diamond nucleation surface. The estimated thermal conductivity of the SiN_x layer and the diamond nucleation layer is 1.9 ± 0.4 W/m-K and 3 W/m-K, respectively. By shrinking both layers, an interfacial thermal resistance approaching the diffuse mismatch prediction is achievable. Based on a transistor thermal model, the combination of high diamond thermal conductivity and low interfacial thermal resistance measured here results in a substantial reduction in device thermal resistance compared to state-of-the-art GaN-on-SiC wafers.

The authors are grateful to J. Anaya Calvo (University of Bristol) and Richard Balmer (Element Six) for helpful discussions in preparing the manuscript. This work was supported by the Engineering and Physical Sciences Research Council (EPSRC) under Grant EP/K024345/1.

[1] D. Francis, F. Faili, D. Babić, F. Ejeckam, A Nurmikko, and H. Maris, Diamond. Rel. Mater. 19(2-3), 229 (2010).
[2] D.C. Dumka, T.M. Chou, F. Faili, D. Francis and F. Ejeckam, IEEE Electron. Lett. 49(20), 1298 (2013).
[3] D. C. Dumka, T. M. Chou, J. L. Jimenez, D. M. Fanning, D. Francis, F. Failia, F. Ejeckama, M. Bernardoni, J. W. Pomeroy, and M. Kuball, in Proceedings of the 34th Annual IEEE Compound Semiconductor Integrated Circuit Symposium, Monterey, USA, 2013, F.4.
[4] J. W. Pomeroy, M. Bernardoni, D. C. Dumka, D. M. Fanning, and M. Kuball, Appl. Phys. Lett. 104(8), 083513 (2014).
[5] J. D. Blevins, G.D. Via, K. Sutherlin, S. Tetlak, B. Poling, R. Gilbert, B. Moore, J. Hoelscher, B. Stumpff, A. Bar-Cohen, J.J. Maurer, A. Kane, in Proceedings of the Compound Semiconductor Manufacturing Technology Conference, Denver, USA, 2014, 105.
[6] J. Kuzmík, S. Bychikhin, D. Pogany, E. Pichonat, O. Lancry, C. Gaquière, G. Tsiakatouras, G. Deligeorgis, and A. Georgakilas, J. Appl. Phys., 109(8), 086106 (2011).
[7] J. Cho, Z. Li, E. Bozorg-Grayeli, T. Kodama, D. Francis, F. Ejeckam, F. Faili, M. Asheghi, and K. E. Goodson, IEEE Trans. Compon., Packag., Manuf. Technol. 3(1), 79 (2013).
[8] A. Manoi, J. W. Pomeroy, N. Killat, and M. Kuball, IEEE Electron Device Lett. 31(12), 1395 (2010).
[9] J. Cho, E. Bozorg-Grayeli, D. H. Altman, M. Asheghi, and K. E. Goodson, IEEE Electron Device Lett. 33(3), 378 (2012).
[10] J. Cho, Y. Li, W. E. Hoke, D. H. Altman, M. Asheghi, and K. E. Goodson, Phys. Rev. B 89(11), 115301 (2014).
[11] A. Sarua, H. Ji, K. P. Hilton, D. J. Wallis, M. J. Uren, T. Martin, and M. Kuball, IEEE Trans. Electron Devices 54(12), 3152 (2007).
[12] J. W. Pomeroy, R. B. Simon, H. Sun, D. Francis, F. Faili, D. J. Twitchen, and M. Kuball, IEEE Electron Device Lett. (2014).
[13] N. Watanabe, T. Kimoto, and J. Suda, J. Appl. Phys. 104(10), 106101 (2008).
[14] S. Wu, PhD. Thesis, University of Rochester, 2007.

[15] M.D. Kamatagi, N.S. Sankeshwar, B.G. Mulimani, Diamond. Rel. Mater. 16(1), 98 (2007).
[16] J. Leitner, A. Strejc, D. Sedmidubský, K. Růžička, Thermochim. Acta 401(2), 169–173 (2003).
[17] V. I. Nepsha, in Handbook of Industrial Diamonds and Diamond Films, edited by Mark A. Prelas, Galina Popovici, and Louis K. Bigelow, (CRC Press, 1997) p. 151.
[18] J. E. Graebner, S. Jin, G. W. Kammlott, Y. H. Wong, J. A. Herb, and C. F. Gardinier, Diamond Relat. Mater. 2(5-7), 1059 (1993).
[19] M. T. Alam, M. P. Manoharan, M. A. Haque, C. Muratore, and A. Voevodin, J. Micromech. Microeng. 22(4), 045001 (2012).
[20] J. Cho, K. K. Chu, P. C. Chao, C. McGray, M. Asheghi, and K. E. Goodson, in Proceedings of the IEEE Intersociety Conference on Thermal and Thermomechanical Phenomena in Electronic Systems, Orlando, USA, 2014, 1186.
[21] S. Bai, Z. Tang, Z. Huang, and J. Yu, IEEE Trans. Ind. Electron. 56(8), 3238 (2009).
[22] M. A. Angadi, T. Watanabe, A. Bodapati, X. Xiao, O. Auciello, J. A. Carlisle, J. A. Eastman, P. Keblinski, P. K. Schelling, and S. R. Phillpot, J. Appl. Phys. 99(11), 114301 (2006).
[23] W. L. Liu, M. Shamsa, I. Calizo, A. A. Balandin, V. Ralchenko, A. Popovich, and A. Saveliev, Appl. Phys. Lett. 89(17), 171915 (2006).
[24] Y. Won, J. Cho, D. Agonafer, M. Asheghi, and K. E. Goodson, in Proceedings of the 34th Annual IEEE Compound Semiconductor Integrated Circuit Symposium, Monterey, USA, 2013, F.1.